Silicon (2022) 14:5319–5331
https://doi.org/10.1007/s12633-021-01300-3

ORIGINAL PAPER

Wear and Frictional Behaviour of Al 7075/FA/SiC Hybrid MMC's Using Response Surface Methodology

Ravi Kumar Mandava [1] · Vajrala Venkata Reddy [2] · Veeravalli Rama Koteswara Rao [3] · K. Srinivasulu Reddy [4]

Received: 3 February 2021 / Accepted: 27 July 2021 / Published online: 16 August 2021

Abstract

In the present research work, an effort was made to study the wear and frictional behaviour of Aluminium metal matrix composite (Al 7075as a base alloy and fly ash (FA) and silicon carbide (SiC) as reinforcements) by using the stir casting method. To carry out this work, the wt.% of reinforcements FA (2.5%, 5%, 7.5% and 10%) and SiC (2.5%, 5%, 7.5% and 10%)5%, 10%, 15% and 20% were used. Initially, the mechanical studies were conducted, and to arrive the mechanical properties obtained at 20 wt.% of FA and SiC. Later on, the composite was fabricated by 20 wt.% of FA and SiC reinforcements were used to check the wear and frictional behaviour on a pin-on-disc machine in dry condition. The dry sliding wear behaviour was carried out at various input parameters such as applied force (10 N, 20 N, and 30 N), sliding velocity (1.5 m/s, 3 m/s, and 4.5 m/s), and sliding distance (1000 m, 2000 m, and 3000 m). Further, a scanning electron microscope (SEM) was used to study the microstructural behaviour of the composites and the worn surfaces during wear test. A response surface methodology (RSM) is a reasonable and accurate method for conducting the experiments and identifying the optimal wear parameters. Moreover, the RSM helped to identify the most significant factor, which was the influence on the wear rate. Finally, it was found that the applying load is the utmost significant factor that affects wear rate. The sliding velocity and sliding distance are found to have less influence on the performance indicator.

Keywords Al 7075 · Fly ash · Silicon carbide · RSM · Wear rate

1 Introduction

In recent years, the usage of aluminum metal matrix composites (AMMC's) are increasing in aerospace, naval, and automobile industries due to their superior mechanical, tribological, microstructural properties and lightweight. In general, AMMC's are modified based on the said application and numerous benefits, namely low coefficient of friction, adequate wear resistance, superior strength-to-weight ratio, and high corrosion resistance. Therefore, wear is a significant parameter duly considered while designing and manufacturing any machine elements and ensuring the performance is improved [7, 21]. Through the particle dispersion, solid lubricant in the aluminum alloy can display better potential for wear resistance. Moreover, graphite is added in aluminum alloy because of better properties like low friction, chemical inertness, film-forming ability, and inherent absence. The addition of graphite particulates with aluminum alloys can diminish the wear rate and reduce flexural strength and hardness [12]. Most researchers add

✉ Ravi Kumar Mandava
ravikumar1013@gmail.com

Vajrala Venkata Reddy
vajram22@gmail.com

Veeravalli Rama Koteswara Rao
vrkrao112880@gmail.com

K. Srinivasulu Reddy
k.srinivasulureddy@gmail.com

[1] Department of Mechanical Engineering, MANIT Bhopal, Bhopal 462003, India

[2] School of Mechanical and Industrial Engineering, Diredawa University, 1362 Diredawa, Ethiopia

[3] Department of Mechanical Engineering, R.V.R & J.C. College of Engineering, Guntur 522006, India

[4] Department of Mechanical Engineering, Sreenidhi Institute of Science and Technology, Hyderabad 501301, India

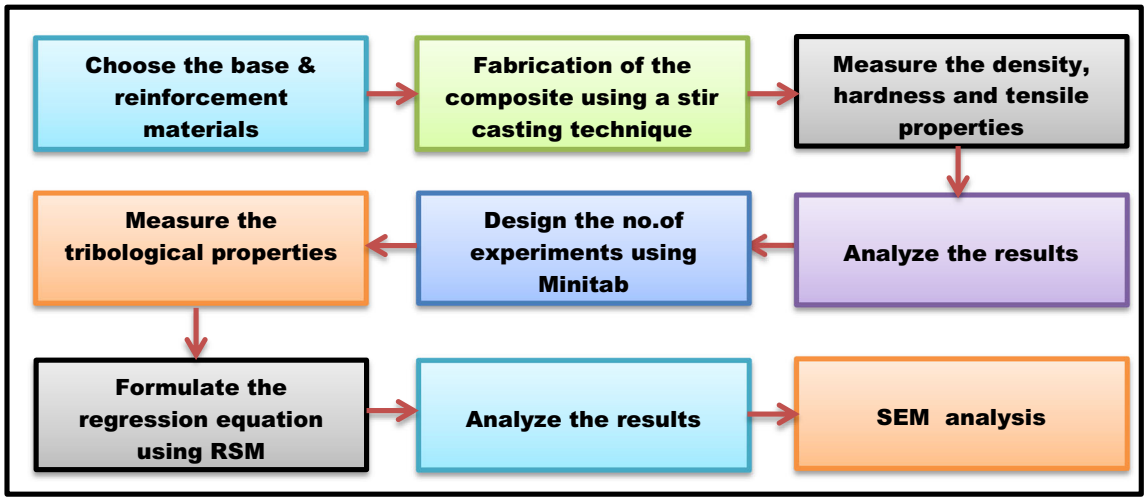

Fig. 1 Graphical flow chart showing the step-by-step process of experimental methodology

both ceramics and lubricants to develop hybrid composites to overcome the above problem, leading to better mechanical and tribological properties [17, 18, 26, 27, 30]. Al 7075 has owing the high strength and greater potential in dry sliding wear applications [2, 9]. Many researches [19, 24, 29] were done to study the wear behaviour of Al 7075 alloy reinforced with various ceramic reinforcements like silicon carbide (SiC), titanium carbide (TiC), alumina (Al_2O_3), graphite (Gr), titanium boride (TiB_2), etc. An investigation was conducted on the effect of SiC and its particle size of Al 7075-SiC composites and observed a significant enhancement in the composite mechanical and tribological properties of the composite when compared with base material [16]. Added to this a study [5] was carried out on the performance of wear on Al 7075 reinforced with Al_2O_3 composites and it was found that the adding of ceramics improves the wear resistance.

Further, an investigation [3] has been carried out on Al 7075 reinforced with B_4C composites and observed that the enhancement in hardness and wear resistance, but there is a reduction in COF. Baskaran et al. [6] discussed the wear behaviour of Al 7075 reinforced with TiC and it was observed that the behaviour of wear reductions under dry conditions. Ranjan et al. [14] fabricated a composite using Al 7075 reinforced with TiB_2 particles and identified the tribological behaviour on developed composites, and they mentioned higher wear resistance with increasing the TiB_2 particles. Recently, Idrisi et al. [11] fabricated a composite by Al6061 reinforced with SiC particles in various fractions using an ultrasonic vibration-based stir casting process. After adding SiC particles, the author's observed the density, hardness, tensile, and compressive strength increased compared to the traditional stir casting process. In [10], the authors reported the hardness decreased with an increase in the graphite percentages within aluminum matrix. Moreover, Akhlaghi et al. [1] fabricated a composite by varying the Gr from 5% to 20% and Al2024 as a matrix. After the experiments conducted, the authors reported that the composite's hardness and toughness reduced after adding the Gr as reinforcement. Further, Baradeswaranet al. [4] discussed after adding the Gr with Al 7075, the hardness decreased, whereas the tensile strength was found increasing. In [15], Mohankumar et al. fabricated a composite with Al 359 as a matrix and B_4C and fly ash as the reinforcements using the stir casting technique. They discussed the hardness, increase in tensile strength, and increase in wear resistance after adding fly ash and B_4C content. Dipankar et al. [8] fabricated a composite with the base metal Al 2024 and different weight percentages of SiC particulates and conducted the mechanical and tribological tests. The authors concluded that because of SiC particulates, the mechanical and tribological properties improved than the matrix alloy. In [22], the authors discussed about the dry sliding wear behaviour of Al 6082 reinforced with red mud particles. The authors observed that with higher content of red mud particles, the hardness, yield, and tensile strength increased, where as a reduction in the impact strength was observed. Further, due to the involvement of high red mud particles, the wear rate of the specimens decreased with an increase in the sliding distance. Later on, Samal et al. [20] studied the mechanical and sliding wear properties of TiC reinforced AA5052 composites. The mechanical properties enhanced with excellent interfacial bonding and uniform dispersion, while the composites exhibited higher wear resistance than the base alloy.

Table 1 Chemical composition of Al 7075

Zn	Cu	Mg	Si	Cr	Mn	Fe	Pb	Sn	Ti	Al
5.6	1.3	2.4	0.4	0.18	0.3	0.5	0.03	0.012	0.2	89

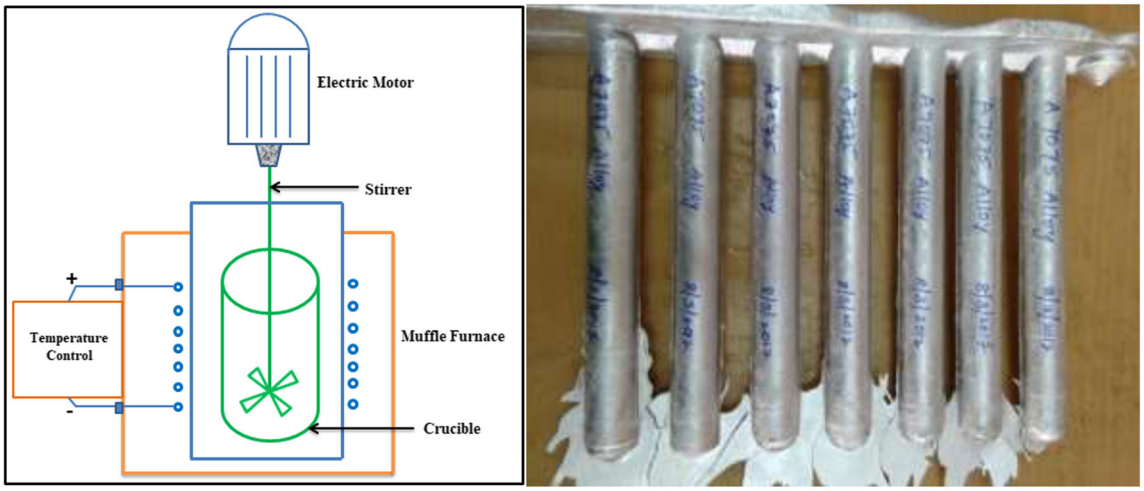

Fig. 2 Schematic diagram showing (**a**) stir casting process and (**b**) casted specimens

Therefore, the current research work is to develop the commercially based Al 7075 reinforced with SiC and fly ash powder-based hybrid composites using the stir casting technique. Further, mechanical properties such as hardness, tensile strength, and tribological characteristics such as wear rate and coefficient friction were studied with respect to the SiC and FA content. RSM has been used for modeling the process parameters (i.e. applying a load, sliding speed, and sliding distance) and planning the number of experiments. The literature study observed that most of the alloys chosen as matrices had been the aluminium alloys; some studies have been reported on the 7xxx series alloys reinforced with SiC, TiC, Al_2O_3, Gr and TiB_2 particles. Significantly less attention has been given to the AA 7075 alloy matrix composites, which have the highest hardness among all Al alloys. Therefore, in the present investigation, SiC and FA particles were used as reinforcements for an aluminium (AA 7075) alloy hybrid metal matrix composite under heat-treated conditions using Response Surface Methodology. The complete flow chart of the present research work is shown in Fig. 1.

2 Materials and Methods

In the present section, the chemical composition of the base alloymaterials, fabrication of the composite, instruments required to conduct the mechanical and tribological tests, and the response surface methodology used for modeling and analysis of the problem are discussed.

2.1 Materials and Instruments

The matrix Al 7075 the reinforcement's fly ash and silicon carbide were procured from Venuka Engineering Private Limited, Hyderabad. The composites were prepared using a stir casting process. The mechanical properties such as hardness and tensile strength of the fabricated composites were measured on a Vickers hardness tester and Universal Testing Machine (UTM). The tribological properties such as wear and coefficient of friction were measured on pin-on-disc apparatus and the scanning electron micrographs (SEM's) were taken

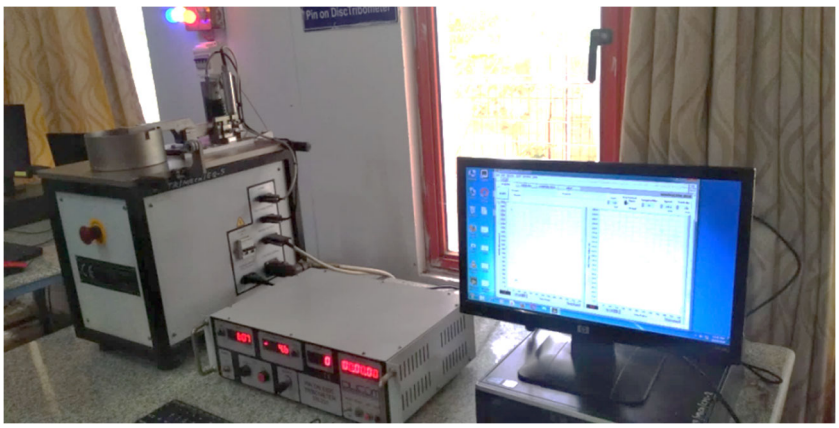

Fig. 3 Pin-on-disc apparatus

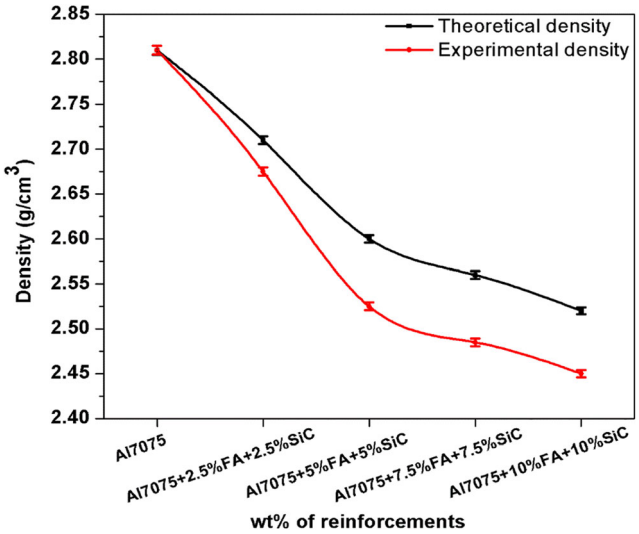

Fig. 4 Variation of density with wt.% of reinforcements

from a scanning electron microscope. Further, the chemical composition of the matrix Al 7075 alloy is given in Table 1.

2.2 Fabrication of the Composite

Al 7075 as a matrix and the reinforcements of 2.5%, 5%, 7.5%, and 10% of fly ash and silicon carbide prepared a composite using stir casting (ref. Figure 2 (a)). Nearly 1000 g of Al 7075 alloy small blocks are placed in a graphite crucible and melted up to the temperature of 850 °C. After the complete melting of aluminum, a stirrer was introduced into the crucible for mixing the reinforcements uniformly. The weight percentages such as 2.5%, 5%, 7.5%, and 10% of fly ash and silicon carbide powder were introduced into the crucible to prepare composite. The stirrer was rotated at 500 ± 10 rpm for 5 min, and it was made by stainless steel sustained at 850 °C temperature. The stirring was continued until it was to ensure proper mixing of reinforcements

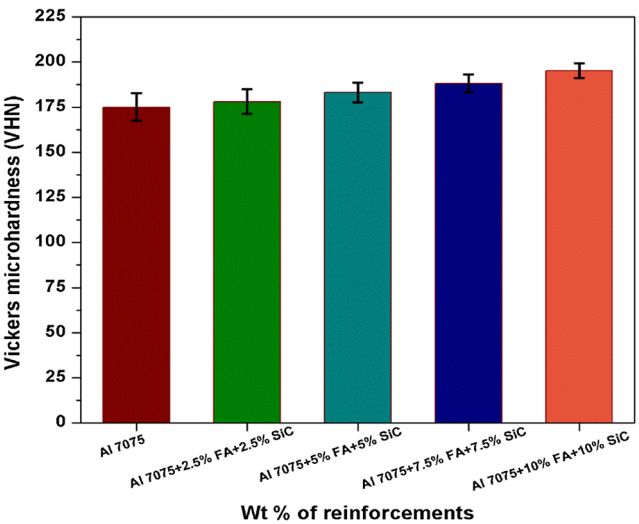

Fig. 5 Graph showing the variation of Vickers microhardness

in a matrix. After completion of adequate mixing, the liquid metal was poured into a preheated mild steel mould. Further, the obtained composite specimens are shown in Fig. 2 (b) were kept under T_6 heat-treated conditions for conducting the hardness, tensile strength, and wear tests.

2.3 Density Test

Measurement of density is one of the important properties to identify the porosity levels of the Al 7075 alloy and fabricated composite specimens. The experimental and theoretical densities were calculated to determine the porosity level in the base alloy and fabricated composites. The Archimedes principle (Eq. (1)) is used to determine the experimental density values, and the theoretical density values were determined by rules of mixtures (Eq. (2)).

$$\rho_{\exp} = \frac{Mass}{Volume} \tag{1}$$

$$\rho_{th} = \rho_m V_m + \rho_r V_r \tag{2}$$

2.4 Hardness and Tensile Test

Once the composites were prepared, the specimens are prepared for the hardness tests as per ASTM E10 standards. Moreover, determining the hardness value is an essential parameter for all fabricated composites. The conventional Vickers microhardness tester with load 1 kg was used to measure the hardness values for both base and fabricated composite materials at room temperature. The test was conducted at room temperature (28 °C) and the measurement of hardness was taken at five different places on each sample to obtain an average value of hardness. Further, the tensile specimens were machined into a cylindrical shape as per ASTM E8 standards. The prepared specimens were tested on a universal tensile testing machine at room temperature. For obtaining the accurate result, three samples were tested in each category, and the average value is reported in this study.

2.5 Wear Test

To measure the wear properties on a pin-on-disk testing machine (Fig. 3) initially, the developed composite specimens were prepared with a diameter and height of 8 mm and 50 mm, respectively. The counter face of the disc was made up of EN31 hardened steel with a thickness and diameter of 5 mm and 90 mm, respectively. Before experimenting, both sides of the specimens were polished by using different sizes of emery papers. Further, the wear test was conducted by varying the sliding speed of 1.5–4.5 m/s, the sliding distance of 1000–3000 m, and the applied load of 10–30 N under ambient conditions. While experimenting before and after each test the weight of the specimens was measured using a weighing machine with a precision of 0.001 mg.

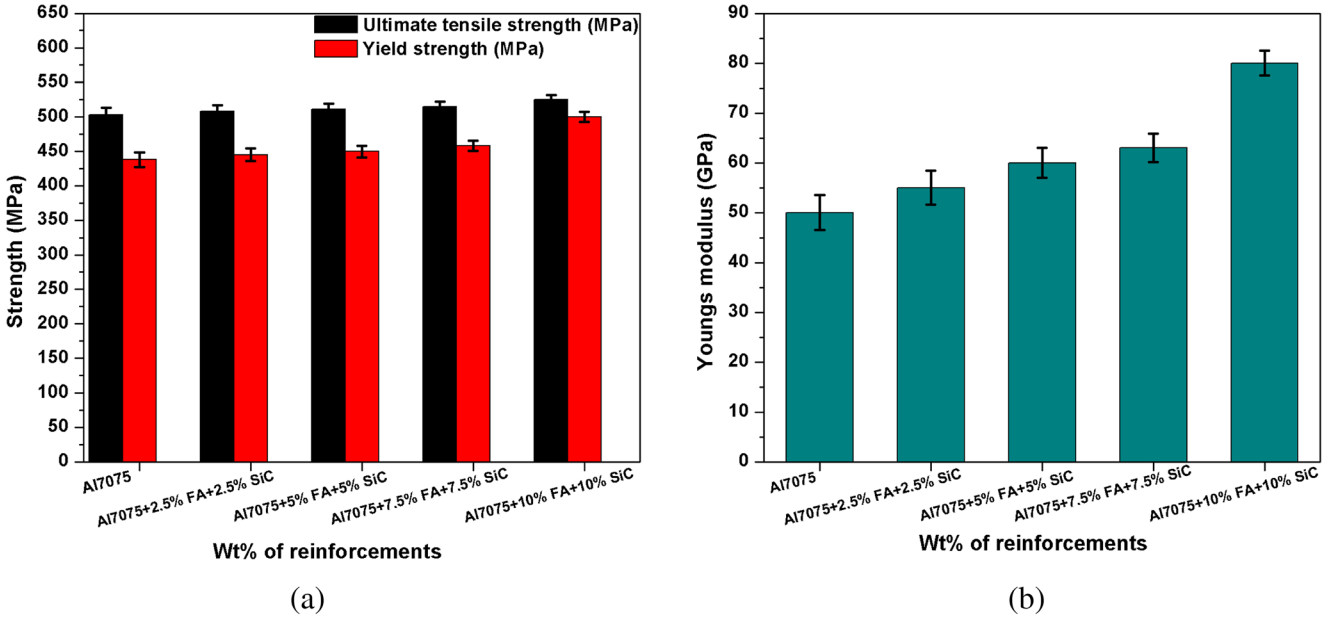

Fig. 6 Graph Showing the variation of (**a**) tensile and yield strength, (**b**) young's modulus

The wear rate was calculated using the difference between the volumetric loss per unit sliding distance earlier and later of each test. Moreover, normal force, friction force, and sliding surfaces of contact were continuously recorded by a load cell to measure the COF. The morphologies of the worn surfaces of the tested samples were examined using SEM to study the wear mechanism for the composites.

2.6 Response Surface Methodology (RSM)

RSM adopts both mathematical and statistical techniques, which are helpful to determine both the modeling and analysis of the problem. Moreover, this method will also help estimate the coefficients, study the responses based on the combinations, fit with the experimental data, predict the response, and check the fitted model's adequacy [28]. The sliding speed, sliding distance, and applying load are selected as independent variables and the wear rate and coefficient friction were treated as response variables. The initial input variable sliding speed was varied between the two levels 1.5 and 4.5 m/s relatives to the center point 3 m/s. The second input variable, the sliding distance, varied between the two levels 1000 and 3000 m relative centre point 2000 m. Further, the third input variable, applying load, varied between the 10 and 30 N with the centre point 20 N. Alongside, the wear rate and COF are the dependent variables that are to be examined with respect to the input variables.

Table 2 Input levels of wear parameters

S.No.	Parameters	Levels		
		Low (−1)	Medium (0)	High (+1)
1	Applying load (N)	10	20	30
2	Sliding speed (m/s)	1.5	3	4.5
3	Sliding distance (m)	1000	2000	3000

3 Results and Discussion

3.1 Density

The variation of the experimental and theoretical densities of the composite materials are shown in Fig. 4. It was observed that the density of the fabricated composite (after adding the reinforcements such as, fly ash and SiC) was low compared to the base material. Moreover, it was observed that the density decreases when the percentage of reinforcements increases. Similar trends were also observed the previous researchers [8, 20, 22]. Further, the density of the experimental was low compared to the theoretical density. It may be due to the porosity increases while fabricating the composite.

3.2 Microhardness

The surface of the fabricated hybrid composite samples and base material were prepared to determine the hardness value. Figure 5 shows the Vickers microhardness values for both base and composites. It was observed that the hardness of the fabricated composite specimens was increased compared to the base aluminum 7075 alloys. Moreover, it is clearly understood that the hardness of the fabricated composite increased while increasing the weight percentage of SiC and fly ash reinforcements. The hardness of the base material to composites increased from 175 VHN to 190 VHN. It may be

Table 3 Design matrix and experimental wear result

Std Order	Run Order	Sliding speed (m/s)	Sliding distance (m)	Applying load (N)	Wear rate (mm^3/m)	Coefficient of friction
1	19	1.5	1000	10	0.360275	0.950
2	2	4.5	1000	10	0.244166	0.490
3	13	1.5	3000	10	0.189907	0.625
4	6	4.5	3000	10	0.126605	0.475
5	14	1.5	1000	30	0.678240	0.410
6	17	4.5	1000	30	0.434074	0.250
7	11	1.5	3000	30	0.094227	0.410
8	4	4.5	3000	30	0.067098	0.300
9	7	1.5	2000	20	0.501898	0.480
10	8	4.5	2000	20	0.257731	0.180
11	5	3.0	1000	20	0.596851	0.400
12	12	3.0	3000	20	0.343642	0.350
13	15	3.0	2000	10	0.406944	0.875
14	20	3.0	2000	30	0.464998	0.406
15	16	3.0	2000	20	0.458000	0.426
16	1	3.0	2000	20	0.484000	0.419
17	18	3.0	2000	20	0.495998	0.405
18	3	3.0	2000	20	0.435500	0.421
19	9	3.0	2000	20	0.444998	0.405
20	10	3.0	2000	20	0.475500	0.416

because fly ash particulates consist of high in silica and alumina, which are hard. The combining effect of SiC and fly ash resists the indention energy, thus causing an enhancement in the hardness. Due to the better strain energy, the hardness of the developed composites is increased at the peripheral of the particles dispersed in the matrix. Therefore, the uniform dispersion of reinforcements causes the enhancement of the hardness and rigidity of the composite.

3.3 Tensile Strength

Figure 6 shows the variation of tensile strength, yield strength, and young's modulus with varying SiC and fly ash. The tensile strength, yield strength, and young's modulus increased with an increase in the SiC and fly ash content and it is significantly greater than the strength of the base alloy. It may be because SiC and fly ash reinforcements exhibit a perfect bonding with Al 7075 alloy, which helps in enduring more loads compared to Al 7075 alloy. The structure and properties of SiC and fly ash particles build a strong interface between matrix to reinforcements and showing better tensile strength.

3.4 Dry Sliding Wear Behaviour

After conducting the mechanical tests the hardness and tensile of the developed hybrid composites were achieved the best results at 10% reinforcements of SiC and fly ash. Further, the dry sliding wear behaviour was conducted at 10% of SiC and fly ash hybrid composites. The central composite design is basically used to design the experiment, develop the models, and analyze the results, which was successfully used previously in many machining and tribological studies [23, 25]. Table 2 shows the input

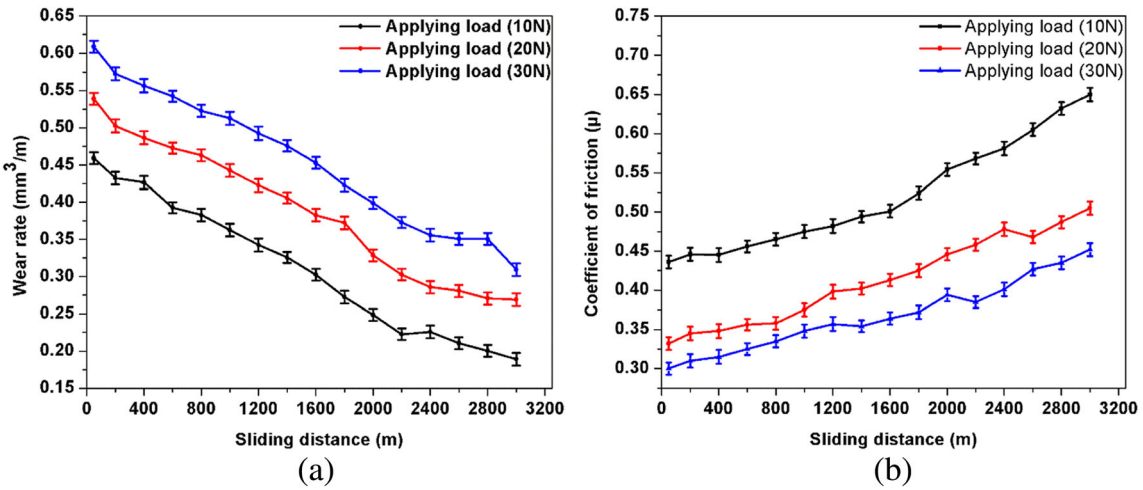

Fig. 7 Variation of wear and frictional behaviour with respect to sliding distance under different load conditions (**a**) wear rate and, (**b**) coefficient of friction

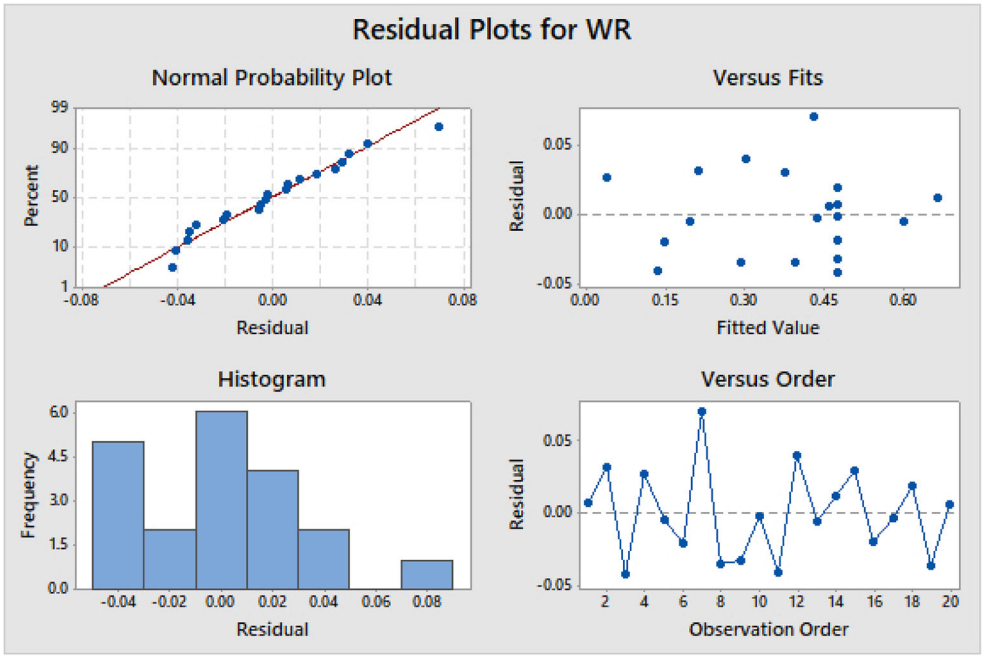

(a)

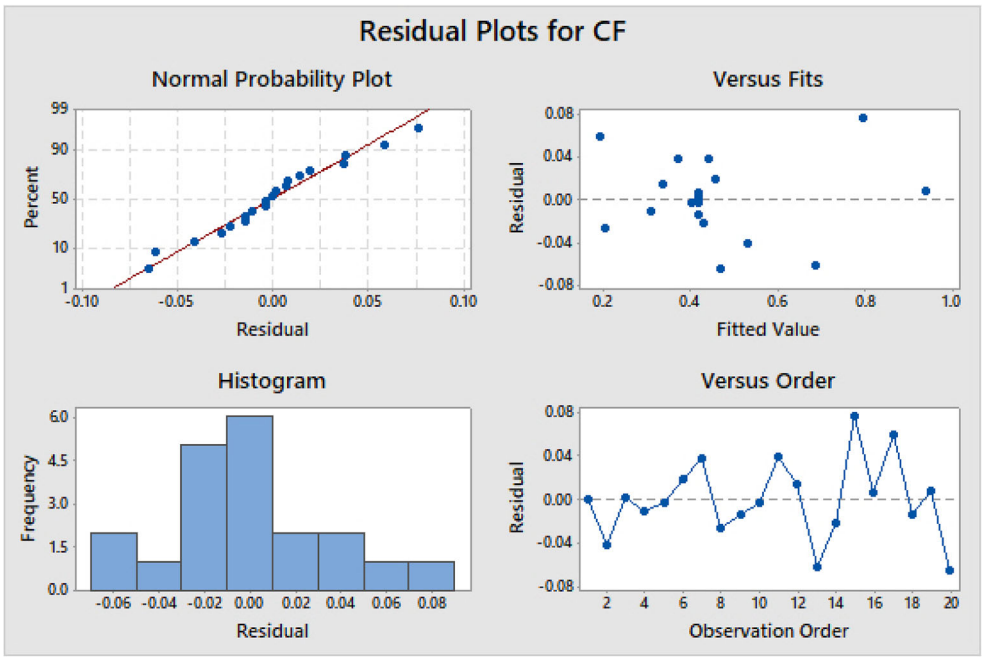

(b)

Fig. 8 Residual plots (**a**) wear rate, and (**b**) coefficient of friction

parameters with their levels used for the current study. Based on the number of input variables and levels (shown in Table 2) the number of experiments were planned for the present study is given in Table 3. The significance values of the coefficients were tested at a 95% confidence level using the MINITAB 16. Later on, the developed mathematical models were established to estimate the wear rate and COF. The mathematical expressions for the hybrid composites are given below.

$$\begin{aligned}\textbf{Wear rate (WR)} = {} & -0.205 + 0.2309\text{*Sliding speed} \\ & + 0.000048\text{*Sliding distance} + 0.0465\text{*Applying load} \\ & -0.0511\text{*Sliding speed*Sliding speed} - 0.000589 \\ & \text{*Applying load*Applying load} + 0.000022 \\ & \text{*Sliding speed*Sliding distance} - 0.000766 \\ & \text{*Sliding speed*Applying load} - 0.000008 \\ & \text{*Sliding distance*Applying load}\end{aligned}$$

$$\begin{aligned}\textbf{Coefficient of friction (CoF)} = {} & 1.880 + 0.0575\text{*Sliding speed} \\ & -0.000022\text{*Sliding distance}-0.1209 \\ & \text{*Applying Load}-0.0421\text{*Sliding speed} \\ & \text{*Sliding speed} + 0.002157\text{*Applying Load} \\ & \text{*Applying Load} + 0.000030\text{*Sliding speed} \\ & \text{*Sliding distance} + 0.00283\text{*Sliding speed} \\ & \text{*Applying Load} + 0.000005 \\ & \text{*Sliding distance*Applying Load}\end{aligned}$$

The Fig. 7 illustrates the wear rate and coefficient of friction of the developed composite specimens with respect to sliding distance under various load conditions from 10 to 30 N. From Fig. 7 (a), the wear rate is high when the sliding distance is small and slow; the wear rate decreased with an increase in the sliding distance. It was obvious that the wear rate is high when the applied load is 30 N compared to 10 N. It may happen the wear rate is more when a high load is applied on the specimen due to the contact area between the specimen and disc is more than the small load. With the increase in the applied load, the surface of the composites undergoing higher temperature condition, which loses its thermal stability and bonding. Therefore, the plastic deformation of the sliding surfaces was more which caused a higher wear rate [13]. Furthermore, an increase in the applied load led to the formation of larger grooves on the specimen surface. These large groves resulted in high deformation with severe wear loss. Overall, the decrease in the wear rate was credited to the composites' higher hardness, which reduced the contact area during the sliding action. Similarly, from Fig. 7 (b), the coefficient of friction is small initially and slowly increases when the sliding distance increases. The continuous sliding action due to the higher sliding distances ensured higher roughness above the surface, increased the contact duration among sliding mating parts, resulting in a higher coefficient of friction. Further, the coefficient of friction is high at 10 N than 30 N, and it may be the reason for less load.

3.5 Testing the Data and Competence of the Model

The normal probability graph of the residuals for wear rate and COF of the fabricated hybrid composites are shown in Fig. 8. It was observed that the residuals were falling on the straight line and the means of errors were distributed normally. Moreover, it can also be confirmed that there was no predictable pattern observed because all the run residues lay on or between the levels. The ANOVA technique was used to test the significance of the established model and the coefficient specifies the goodness of fits of the model. The ANOVA results related to the wear rate and COF for their levels, factors, and their interactions are given in Tables 4 and 5.In the present problem, the value of the coefficient for wear rate ($R^2 = 0.9666$) and coefficient of friction ($R^2 = 0.9610$) indicates that only less than 5% of the total variance. Further, the adjusted coefficient for wear rate (adjusted $R^2 = 0.9365$) and coefficient of friction (adjusted $R^2 = 0.9259$) are high, which means the significance of the model is high. Based on

Table 4 Variance for wear rate

Source	DF	Adj SS	Adj MS	F-Value	*P* Value
Model	9	0.505943	0.056216	32.13	0.000
Linear	3	0.287800	0.095933	54.83	0.000
Speed	1	0.048285	0.048285	27.60	0.000
SD	1	0.222645	0.222645	127.26	0.000
Load	1	0.016871	0.016871	9.64	0.011
Square	3	0.153029	0.051010	29.16	0.000
Speed*Speed	1	0.036419	0.036419	20.82	0.001
SD*SD	1	0.001671	0.001671	0.95	0.352
Load*Load	1	0.009548	0.009548	5.46	0.042
2-Way Interaction	3	0.065113	0.021704	12.41	0.001
Speed*SD	1	0.009102	0.009102	5.20	0.046
Speed*Load	1	0.001055	0.001055	0.60	0.455
SD*Load	1	0.054956	0.054956	31.41	0.000
Error	10	0.017496	0.001750		
Lack-of-Fit	5	0.014747	0.002949	5.36	0.044
Pure Error	5	0.002749	0.000550		
Total	19	0.523439			

Table 5 Variance for coefficient of friction

Source	DF	Adj SS	Adj MS	F-Value	P Value
Model	9	0.600219	0.066691	27.40	0.000
Linear	3	0.419432	0.139811	57.43	0.000
Speed	1	0.139240	0.139240	57.20	0.000
SD	1	0.011560	0.011560	4.75	0.054
Load	1	0.268632	0.268632	110.35	0.000
Square	3	0.131124	0.043708	17.95	0.000
Speed*Speed	1	0.024724	0.024724	10.16	0.010
SD*SD	1	0.006825	0.006825	2.80	0.125
Load*Load	1	0.127926	0.127926	52.55	0.000
2-Way Interaction	3	0.049662	0.016554	6.80	0.009
Speed*SD	1	0.016200	0.016200	6.65	0.027
Speed*Load	1	0.014450	0.014450	5.94	0.035
SD*Load	1	0.019012	0.019012	7.81	0.019
Error	10	0.024344	0.002434		
Lack-of-Fit	5	0.023970	0.004794	64.21	0.000
Pure Error	5	0.000373	0.000075		
Total	19	0.624563			

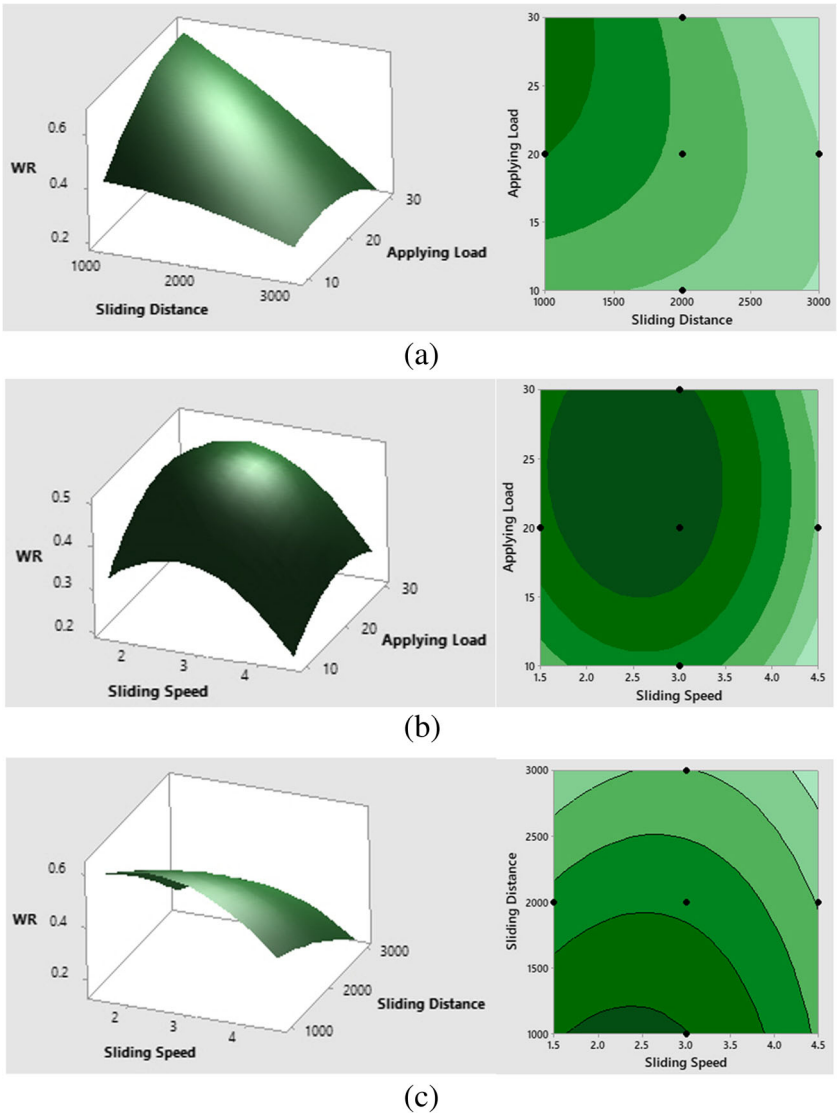

Fig. 9 3D surface and contour plots for predicting the wear rate (**a**) sliding distance vs applying a load, (**b**) sliding speed vs applying load, and (**c**) sliding speed vs sliding distance

the above results, the predicted R^2 value is also better than the adjusted R^2. The ANOVA result of wear rate and coefficient of friction for the developed hybrid composites is shown in Tables 4 and 5 which indicates that the predictability of the developed model for wear rate and coefficient of friction is at a 95% confidence level because the value of p is less than the 0.05 in most of the cases even though the value of p is more than the 0.05 such parameters are not that much influence on the significant level. It was observed that the individual effect of all the three parameters on wear rate is significant, whereas square terms of sliding speed and applied load are also significant. With a *p* value of less than 0.05, the interaction terms of sliding speed, applied load, sliding distance, and speed are significant influences on the wear rate of the composites. Similarly, the individual and square terms of sliding speed and applied load are found to significantly affect the coefficient of friction, whereas all the interaction terms between the input variables influenced the friction coefficient value between the mating sliding parts of composite specimen and rotating disc.

Figures 9 (a), (b), and (c) show the 3D surface and 2D contour plots of the wear rate were plotted from Table 3, to identify the responses of various combinations of independent variables. Figure 9(a) shows initially, the wear rate is higher with an increase in the applying load and is lower with the sliding distance. Later on, the wear rate was decreased with the increase in the sliding distance and applying load. It may be due to the reason at initial due to more applying load the specimen more contact with the disc and resulting in more wear. Moreover, Fig. 9(b) shows the wear rate was low at initial, and slowly wear rate increased when the sliding speed and applying load increases, but the wear rate was low at the end of the sliding speed. Further, Fig. 9(c) shows the wear rate increases when the sliding distance and sliding speed were small and slowly decrease when the sliding speed increases. It was observed that the

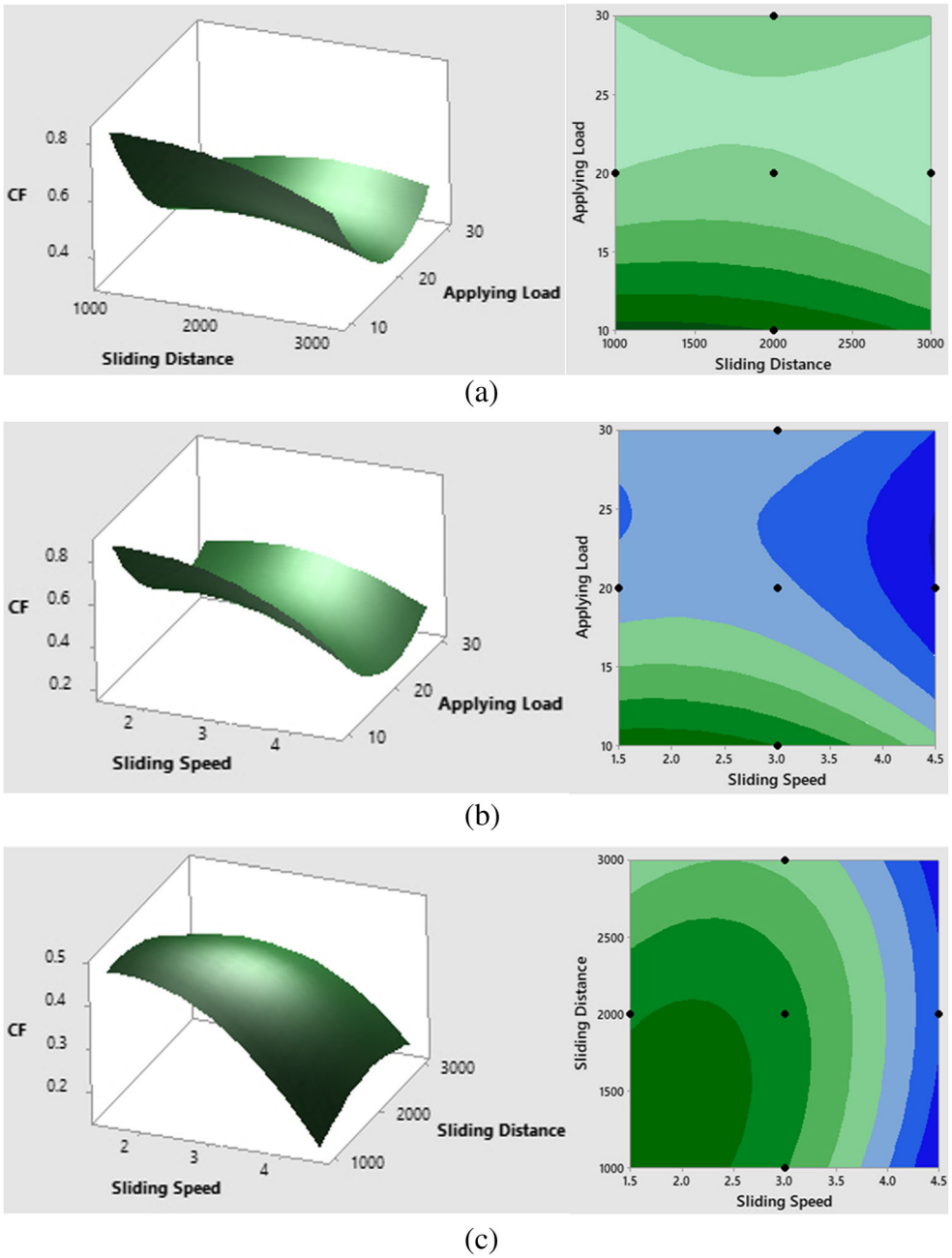

Fig. 10 3D surface and contour plots for predicting the COF (**a**) sliding distance vs applying a load, (**b**) sliding speed vs applying a load, and (**c**) sliding speed vs sliding distance

applying load had the most dominant effect on wear rate concerning sliding distance and sliding speed.

Figures 10(a), (b), and (c) show the 3D surface and 2D contour plots of the COFconcerningthree input variables such as sliding distance, applying load, and sliding speed. From Fig. 10(a) it was observed that the COF is high when the sliding distance is small and the applying load is small. Similarly, from Fig. 10(b) it was obvious that the COF is low when the sliding speed is high concerning applying load. It can be observed that the presence of blue regions shows in the contour plot has the minimum COF. Finally, Fig. 10 (c) shows that it has been observed that the COF is high when sliding speed low but, COF decreases slowly when increasing the sliding speed and distance.

Figure 11 shows the SEM worn surface morphology of the selected specimen with the reinforcement of 10% FA and 10% after SiC. It was noted that the analysis of worn surfaces indicates that the delamination, abrasion, and adhesion mechanisms are leading in this alloy. Further, the delamination, abrasion, and oxidation on wear mechanisms were recognized and examined. Severe surface wear, delamination, peeling of the matrix, grooves, ploughing, scratches were recognized in the composite. Moreover, the aluminum alloy contacts with the EN31 steel disk to form an adhesive layer at the contacting

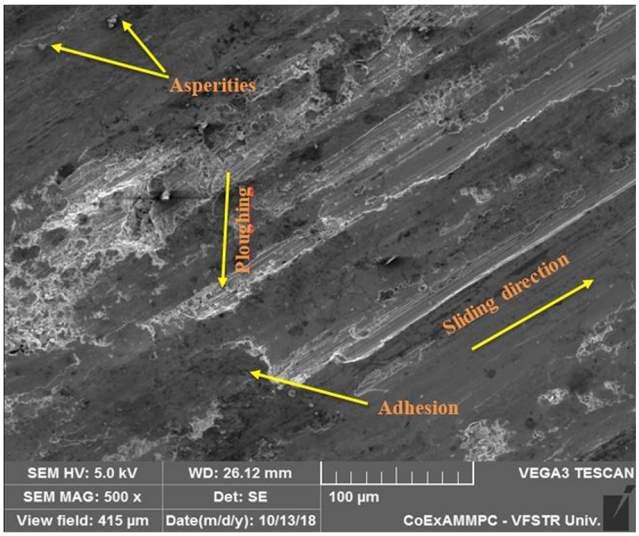

Fig. 11 SEM worn surface morphology image of hybrid composite (Al 7075+ 10%FA + 10% SiC) at 1000 m, 1.5 m/s and 10 N

asperities. It may happen due to the high frictional temperature produced during sliding contact at the interface. Also, in the case of the base alloy, the appearance of shear-like crack characteristics on worn surfaces as represented by arrows reveals that the dominance wear mechanism is delaminated.

The SEM micrographs of the worn surface of Al7075 hybrid composite (10% FA and 10% SiC) under the sliding distance of 1000 m, the sliding velocity of 1.5 m/s, and normal loads of 20 and 30 N at room temperature were shown in Fig. 12 (a) and (b). The composite material at 30 N shows wide and heavy delamination grooves on the surfaces, whereas distinct grooves and ridges running parallel to one another in the sliding direction, as shown with a yellow mark (Fig. 12 (b)), are noticed composites.

3.6 Confirmation Tests

The wear behaviour of Al 7075 + 10%FA + 10%SiC hybrid composite was conducted with various input parameters using a central composite design (Table 3). The confirmatory experimentations were accompaniedto check the precision of the established model and results are displayed in Table 6. Further, the acquired investigational results were well correlated with the predicted results by the developed model. Moreover, it was observed that all the obtained confirmatory results produced an error value which is less than 5% specifies more reliability. Based on the above results, it can be ensured that the developed model was generating good and accurate results. Hence, the developed hybrid composite has been generated superior wear-resistant properties in the long run, which can be suitable for automobile, aerospace, and marine applications.

4 Conclusions

Based on the above experimental work, the subsequent conclusions are made as follows:

- The matrix Al 7075 and reinforcements FA and SiC with different weight percentages vary from 0%, 2.5%, 5%, 7.5%, and 10% were effectively fabricated using the stir casting technique.
- The composite materials exhibit improved mechanical properties with an increase in reinforcement content of 10% of SiC and 10% FA, whereas hardness and tensile strength were found to be 175 to 190 VHN and 498 to 526 MPa, respectively

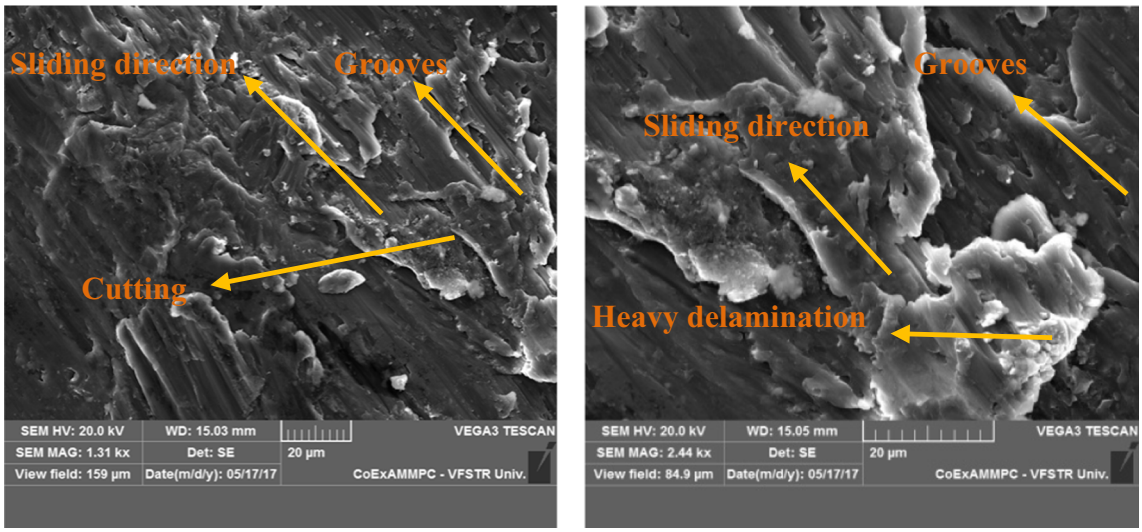

(a) (b)

Fig. 12 Delamination of worn surfaces of Al7075/10% FA/10% SiC Hybrid composites specimens under a load of **(a)** 20 N (b) 30 N at 1000m, 1.5 m/s

Table 6 Conformation results for the developed model

S.No	Sliding speed (m/s)	Sliding distance (m)	Applying load (N)	Experimental		Regression		% of error in WR	% of error in a COF
				WR (mm^3/m)	COF	WR (mm^3/m)	COF		
1	2.0	1400	14	0.5562	0.8017	0.5385	0.7872	3.29	1.84
2	2.5	1800	18	0.6026	0.6954	0.5907	0.6680	2.01	4.10
3	3.5	2200	22	0.5634	0.6124	0.5439	0.5922	3.58	3.41
4	4.0	2600	26	0.4658	0.6499	0.4449	0.6382	4.69	1.83

- Ultimate tensile strength (UTS) and yield strength (Y.S) increases with the increase in percentage of reinforcement. It can be concluded that this behaviour is due to the difference in the elastic constants and load transfer from the matrix to reinforcement. When compared with the matrix material, an increase in UTS was recorded as 5.3% and 11.2%, respectively.
- The wear rate was found to be lower with a higher sliding distance, whereas, with higher applied load, it was observed that the wear rate was increased.
- Central Composite Design was used to estimate the wear rate at various input parameters such as applying load, sliding distance,and sliding speed. The optimal wear rate was attained. The developed model has shown an error estimation of less than 5% which validates the design of wear experiments.
- Moreover, the developed statistical ANOVA effects were revealed that the applying load was contributed toa high wear rate concerning sliding distance and sliding speed.
- Further, the morphology study has been studied for optimal wear rate specimen and identifying the ploughing, asperities, adhesion, and sliding direction.
- Al 7075/SiC/fly ash hybrid composites could be potential material in aerospace, automobile, and marine applications with higher mechanical and wear characteristics.

Acknowledgments Not applicable.

Availability of Data and Materials Yes. If any data is required related to this article, the authors are ready to provide it.

Authors' Contributions First author: He is actively involved in preparing composites, analyzing the results, and writing the article.

Second Author: He is highly involved in testing the mechanical properties and tribological properties.

Third Author: He is actively involved in preparing the composites, testing the materials and writing the article.

Fourth Author: He is actively involved while drafting the article.

Declaration

Ethics Approval and Consent to Participate The authors following the ethics while preparing the material and writing the article.

Consent for Publication Yes. The authors are agreed to publish the work after accepting.

Competing Interests Not Applicable.

References

1. Akhlaghi F, Zare-Bidaki A (2009) Influence of graphite content on the dry sliding and oil-impregnated sliding wear behaviour of Al 2024—graphite composites produced by in situ powder metallurgy method. Wear 266:37–45
2. Bai Y, Guo Y, Li J, Yang Z, Tian J (2017) Effect of Al2O3 nanoparticle reinforcement on the mechanical and high-temperature tribological behaviour of Al-7075 alloy. Proc Inst Mech Eng Part J J Eng Tribol 231:900–909
3. Baradeswaran A, ElayaPerumal A (2013) Influence of B4C on the tribological and mechanical properties of Al 7075-B4C composites. Compos Part B Eng 54:146–1152
4. Baradeswaran A, Perumal AE (2014) Wear and mechanical characteristics of Al 7075/graphite composites. Composites B 56:472–476
5. Baradeswaran A, Elayaperumal A, Franklin Issac R (2013) A statistical analysis of optimization of wear behaviour of Al- Al 2O3 composites using Taguchi technique. Preceding 64(Elsevier):973–982
6. Baskaran S, Anandakrishnan V, Duraiselvam M (2014) Investigations on dry sliding wear behaviour of in situ casted AA7075-TiC metal matrix composites by using Taguchi technique. Mater Des 60:184–192
7. Deuis RL, Subramanian C, Yellup JM (1997) Dry sliding wear of aluminum composites – a review. Compos Sci Technol 57:415–435
8. Dey D, Bhowmik A, Biswas A (2020) Effect of SiC content on mechanical and tribological properties of Al2024-SiC composites. Silicon. https://doi.org/10.1007/s12633-020-00757-y
9. Ebrahimzad P, Ghasempar M, Balali M (2017) Friction stir processing of aerospace aluminum alloy by addition of carbon nanotube. Trans Indian Inst Metals 70:2241–2253
10. Hassan AM, Tashtoush GM, Al-Khalil JA (2007) Effect of graphite and/or silicon carbide particles addition on the hardness and surface roughness of Al-4 wt% Mg alloy. J Compos Mater 41:453–465
11. Idrisi AH, Mourad A-HI (2019) Conventional stir casting versus ultrasonic-assisted stir casting process: mechanical and physical characteristics of AMCs. J Alloys Compd 805:502–508
12. Jun D, Yao-hui L, Si-rong Y, Wen-fang L (2004) Dry sliding friction and wear properties of Al2O3 and carbon short fibers reinforced Al–12Si alloy hybridcomposites. Wear 257:930–940
13. Kumar CR, Malarvannan RR, JaiGanesh V (2020) Role of SiC on mechanical, tribological and thermal expansion characteristics of

B_4C/Talc reinforced Al-6061 hybrid composite. Silicon 12:1491–1500
14. Michael Rajan HB, Ramabalan S, Dinaharan I, Vijay SJ (2014) Effect of TiB2 content and temperature on sliding wear behaviour of AA7075/TiB2 in situ aluminum cast composites. Arch Civ Mech Eng 14:72–79
15. Mohankumar S, Aravind RA, SelvaKumar G, Raja P, Selvam V (2020) Experimental investigation on the tribological -mechanical properties of B4C and fly ash reinforced Al 359 composites. Mater Today: Proc 21:748–754
16. Rao TB (2017) An experimental investigation on mechanical and wear properties of Al 7075/SiCp composites: effect of SiC content and particle size. J Tribol 140:31601–31608
17. Rao RN, Das S (2010) Effect of matrix alloy and influence of SiC particle on the sliding wear characteristics of aluminium alloy composites. Mater Des 31:1200–1207
18. Rao RN, Das S, Mondal DP, Dixit G (2009) Dry sliding wear behaviour of cast high strength aluminium alloy (Al–Zn–Mg) and hard particle composites. Wear 267:1688–1695
19. Ruiz-Andres M, Conde A, De Damborenea J, Garcia I (2015) Wear behaviour of aluminum alloys at slow sliding speeds. Tribol Trans 58:955–962
20. Samal P, Vundavilli PR, Meher A, Mahapatra MM (2019) Influence of TiC on dry sliding wear and mechanical properties of in situ synthesized AA5052 metal matrix composites. J Compos Mater 53(28–30):4323–4336
21. Samal P, Vundavilli PR, Meher A, Mahapatra MM (2020) Recent progress in aluminum metal matrix composites: a review on processing, mechanical and wear properties. J Manuf Process 59:131–152
22. Samal P, Mandava RK, Vundavilli PR (2020) Dry sliding wear behaviour of Al 6082 metal matrix composites reinforced with red mud particles. SN Appl Sci 2(2):1–11
23. Samal P, Babu DM, Kiran SV, Surekha B, Vundavilli PR, Mandal A (2020) Study of microstructural and machining characteristics of hypereutectic Al-Si alloys using wire-EDM for photovoltaic application. Silicon. https://doi.org/10.1007/s12633-020-00742-5
24. Shanmughasundaram P (2015) Statistical analysis on the influence of heat treatment, load, and velocity on the dry sliding wear behaviour of aluminum alloy 7075. Mater PhysMech 118–124
25. Surekha B, Lakshmi TS, Jena H, Samal P (2021) Response surface modelling and application of fuzzy grey relational analysis to optimise the multi response characteristics of EN-19 machined using powder mixed EDM. Aust J Mech Eng 19(1):19–29
26. Toptan F, Kilicarslan A, Karaaslan A, Cigdem M, Kerti I (2010) Processing and microstructural characterization of AA 1070 and AA 6063 matrix B4Cp reinforced composites. Mater Des 31:87–91
27. Vettivel SC, Selvakumar N, Vijay PP (2012) Mechanical behaviour of sintered Cu-5% W nanocomposite. Procedia Eng 38:2874–2880
28. Vettivel SC, Selvakumar N, Narayanasamy R, Leema N (2013) Numerical modeling, prediction of Cu–W nanopowder composite in drysliding wear condition using response surface methodology. Mater Des 50:977–996
29. Yang Z-R, Sun Y, Li X-X, Wang S-Q, Mao T-J (2015) Dry sliding wear performance of 7075 Al alloy under different temperatures and load conditions. Rare Met 1–6. doi: 10.1007/s12598-015-0504-7
30. Zhan Y, Zhang G (2006) The role of graphite particles in the high-temperature wear of copper hybrid composites against steel. Mater Des 27:79–84